Lecture notes
Breakup of cylindrical jets
Singularities and self-similar solutions

BY STEPHANE POPINET AND ARNAUD ANTKOWIAK

June 8, 2011

Table of contents

1 Equations of motion for axisymmetric jets

Following Eggers and Dupont (1994), we will derive approximate equations of motion valid in the limit of slender jets i.e. jets for which the radial dimensions are much smaller than the longitudinal dimensions.

We start by writing the full equations of motion for an incompressible viscous fluid in cylindrical (axisymmetric) coordinates. The equations for the two components of momentum can be written

$$\partial_t u_r + u_r\,\partial_r u_r + u_z\,\partial_z u_r = -\frac{1}{\rho}\,\partial_r p + \nu\left(\partial_{r^2}^2 u_r + \partial_{z^2}^2 u_r + \frac{1}{r}\,\partial_r u_r - \frac{u_r}{r^2}\right) \tag{1}$$

$$\partial_t u_z + u_r\,\partial_r u_z + u_z\,\partial_z u_z = -\frac{1}{\rho}\,\partial_z p + \nu\left(\partial_{r^2}^2 u_z + \partial_{z^2}^2 u_z + \frac{1}{r}\,\partial_r u_z\right) - g \tag{2}$$

For an incompressible fluid, mass conservation is identical to volume conservation and can be written

$$\partial_r u_r + \frac{u_r}{r} + \partial_z u_z = 0 \tag{3}$$

In the case of fluid motion with a free-surface (i.e. the gas-liquid interface of the jet), the free-surface boundary conditions must also be verified i.e.

- interfacial stresses

$$\boldsymbol{n}\cdot\boldsymbol{\sigma}\cdot\boldsymbol{n} = -\sigma\kappa$$
$$\boldsymbol{n}\cdot\boldsymbol{\sigma}\cdot\boldsymbol{t} = 0$$

- kinematic boundary condition

$$\frac{d\mathcal{F}}{dt} = 0$$

where the interface is defined by $\mathcal{F}(\boldsymbol{x}, t) = 0$.

In the case of slender jets, we can choose to define the interface as

$$\mathcal{F}(\boldsymbol{x}, t) = r - h(z, t) = 0$$

With this choice of parameterisation, the unit tangent and normal vectors are given by

$$\boldsymbol{t} \;=\; \frac{1}{\sqrt{1+h'^2}} \begin{pmatrix} h' \\ 1 \end{pmatrix}$$

$$\boldsymbol{n} \;=\; \frac{1}{\sqrt{1+h'^2}} \begin{pmatrix} 1 \\ -h' \end{pmatrix}$$

The normal component of the stress can then be written

$$\boldsymbol{n}\cdot\boldsymbol{\sigma}\cdot\boldsymbol{n} \;=\; \frac{1}{1+h'^2} \begin{pmatrix} 1 \\ -h' \end{pmatrix} \begin{pmatrix} \sigma_{rr} & \sigma_{rz} \\ \sigma_{rz} & \sigma_{zz} \end{pmatrix} \begin{pmatrix} 1 \\ -h' \end{pmatrix}$$

$$=\; \frac{1}{1+h'^2}\left(\sigma_{rr} - 2\,h'\,\sigma_{rz} + h'^2\,\sigma_{zz}\right)$$

$$=\; -p + \frac{2\,\mu}{1+h'^2}\left(\partial_r u_r - h'\left(\partial_r u_z + \partial_z u_r\right) + h'^2\,\partial_z u_z\right)$$

which gives the boundary condition

$$-p + \frac{2\,\mu}{1+h'^2}\left(\partial_r u_r - h'\left(\partial_r u_z + \partial_z u_r\right) + h'^2\,\partial_z u_z\right) = -\sigma\,\kappa \quad\text{at}\quad r=h \tag{4}$$

Similarly, the tangential stress condition can be written

$$\boldsymbol{n}\cdot\boldsymbol{\sigma}\cdot\boldsymbol{t} = \frac{\mu}{1+h'^2}\left(2\,\partial_r u_r\,h' + \left(\partial_r u_z + \partial_z u_r\right)\left(1 - h'^2\right) - 2\,h'\,\partial_z u_z\right) = 0 \quad\text{at}\quad r=h \tag{5}$$

Finally, the kinematic boundary condition can be expressed

$$\frac{d\mathcal{F}}{dt} = \partial_t h - u_r + u_z\,\partial_z h = \partial_t h - u_r + u_z\,h' = 0 \quad\text{at}\quad r=h \tag{6}$$

The full axisymmetric problem is thus described by six coupled equations!

1.1 Equations of motion valid in the limit of slender jets

The previous set of equations is clearly too complex to be amenable to analytical treatment. Simplified equations of motion can be obtained in the limit of slender jets. If the characteristic radial dimensions of the jet are much smaller than its longitudinal dimensions, it is natural to assume that quantities are almost uniform along the radial dimension. This suggests describing all quantities using Taylor series expansions in r. For example, the longitudinal component of the velocity could be written

$$u_z(r,z,t) = u_0(z,t) + r\,u_1(z,t) + r^2\,u_2(z,t) + r^3\,u_3(z,t) + \ldots$$

This can be further simplified by using the symmetries of the solution. For example the longitudinal component of the velocity must be symmetrical about the axis of revolution i.e. we have

$$\partial_r u_z = 0 \quad\text{at}\quad r=0$$

u_z must thus be an even function of r, so that

$$u_{2n+1}(z,t) = 0 \text{ for all } n$$

All quantities can be developed using this scheme. For example the radial component of the velocity can be written

$$u_r(r,z,t) = r\,u_{r_1}(z,t) + r^3\,u_{r_3}(z,t) + \ldots$$

where we have used the (odd) symmetry of u_r about the axis of revolution.

For slender jets we will use the fact that r is small so that

$$1 \gg r \gg r^2 \gg r^3 \gg \ldots$$

to derive an *asymptotic expansion* of the equations of motion. For example, if we take the continuity equation (3), we have to second-order in r

$$\partial_r u_r + \frac{u_r}{r} + \partial_z u_z = u_{r_1} + 3\,r^2\,u_{r_3} + u_{r_1} + r^2\,u_{r_3} + u_0' + r^2\,u_2' + O(r^3) = 0$$

The leading-order term then gives

$$u_{r_1} = -\frac{1}{2}\,u_0'$$

and to second-order in r

$$u_{r3} = -\frac{1}{4}u_2'$$

which can be generalised to arbitrary order

$$u_r(r,z,t) = -\frac{1}{2}u_0'\,r - \frac{1}{4}u_2'\,r^3 - \ldots - \frac{1}{2n+2}u_{2n}'\,r^{2n+1} + O(r^{2n+3}) \tag{7}$$

We have thus used the continuity equation to eliminate one of the unknown in the system (u_r).

In a similar manner, if we develop the (even-symmetric) pressure as

$$p(r,z,t) = p_0(z,t) + r^2\,p_2(z,t) + O(r^3)$$

we can write the equation for the longitudinal component of the momentum (2) as

$$\partial_t u_z + u_r\,\partial_r u_z + u_z\,\partial_z u_z \;=\; -\frac{1}{\rho}\partial_z p + \nu\left(\partial_{r^2}^2 u_z + \partial_{z^2}^2 u_z + \frac{1}{r}\partial_r u_z\right) - g$$

$$\partial_t u_0 + u_0\,u_0' + O(r) \;=\; -\frac{1}{\rho}p_0' + \nu\,(2\,u_2 + u_0'' + 2\,u_2) - g + O(r) \tag{8}$$

This is clearly not sufficient to fully describe u_z at this order. One needs to add the boundary conditions on the free-surface (4), (5) and (6). To first order, the boundary condition on the normal stress can be written

$$-p + \frac{2\,\mu}{1 + h'^2}\left(\partial_r u_r - h'\left(\partial_r u_z + \partial_z u_r\right) + h'^2\,\partial_z u_z\right) = -\sigma\,\kappa \quad \text{at} \quad r = h$$

$$-p_0 + \frac{2\,\mu}{1 + h'^2}\left(-\frac{1}{2}u_0' - h'\,u_1 + h'^2\,u_0'\right) + O(r) = -\sigma\,\kappa \quad \text{at} \quad r = h$$

This can be further simplified by noting that the slender jet limit implies $h' \ll 1$, so that

$$p_0 + \mu\,u_0' + O(h) + O(h') = \sigma\,\kappa$$

Similarly, the tangential stress boundary condition (5) can be written

$$2\,\partial_r u_r\,h' + \left(\partial_r u_z + \partial_z u_r\right)\left(1 - h'^2\right) - 2\,h'\,\partial_z u_z = 0 \quad \text{at} \quad r = h$$

$$-2\,\frac{1}{2}u_0'\,h' + \left(2\,r\,u_2 - \frac{1}{2}u_0''\,r\right) - 2\,h'\,u_0' + O(r^2) + O(h^2) = 0 \quad \text{at} \quad r = h$$

$$-3\,u_0'\,h' + 2\,h\,u_2 - \frac{1}{2}u_0''\,h + O(h^2) + O(h'^2) = 0$$

These two boundary conditions can then be used to close the momentum equation (8) as

$$\partial_t u_0 + u_0\,u_0' + O(r) \;=\; -\frac{1}{\rho}p_0' + \nu\,(4\,u_2 + u_0'') - g$$

$$= -\frac{\sigma}{\rho}k' + 2\,\nu\,u_0'' + 4\,\nu\,u_2 - g$$

$$= -\frac{\sigma}{\rho}k' + 2\,\nu\,u_0'' + 2\,\nu\left(3\,u_0'\,h'/h + \frac{1}{2}u_0''\right) - g$$

$$= -\frac{\sigma}{\rho}k' + 3\,\nu\,u_0'' + 6\,\nu\,\frac{u_0'\,h'}{h} - g$$

$$= -\frac{\sigma}{\rho}k' + 3\,\nu\,\frac{(u_0'\,h^2)'}{h^2} - g \tag{9}$$

to which must be added the kinematic boundary condition (6)

$$\partial_t h - u_r + u_z\,h' = 0 \quad \text{at} \quad r = h$$

$$\partial_t h + \frac{1}{2}u_0'\,h + u_0\,h' + O(h^2) = 0 \tag{10}$$

Using the assumption of a slender jet to perform an asymptotic expansion, we have thus reduced the full set of partial-differential axisymmetric equations (1), (2), (3), (4), (5) and (6) to just one ordinary differential equation (9) for u_z with boundary condition (10) and a diagnostic equation (7) for u_r.

2 Linear stability analysis

What is the cause of the breakup of a jet into a stream of droplets? As first observed by Plateau, a cylinder is not the geometry which minimises the total surface area for a given volume (and thus it does not minimise the total surface energy due to surface tension). If we assume that a cylinder of length L and diameter R is divided into n identical droplets, each droplet will have a radius

$$r = \left(\frac{3\,R^2\,L}{4\,n} \right)^{\frac{1}{3}}$$

so that the total surface area for this configuration will be

$$n\,4\,\pi \left(\frac{3\,R^2\,L}{4\,n} \right)^{\frac{2}{3}} = 4\,\pi \left(\frac{3}{4} \right)^{\frac{2}{3}} n^{\frac{1}{3}}\,R^{\frac{4}{3}}\,L^{\frac{2}{3}}$$

The ratio of this surface area to the surface area of the initial cylinder is thus

$$2 \left(\frac{3}{4} \right)^{\frac{2}{3}} n^{\frac{1}{3}} \left(\frac{R}{L} \right)^{\frac{1}{3}}$$

which is valid only in the limit of slender jets (i.e. $R/L \to 0$) as we have neglected the area of the ends of the cylinder. The total surface area of the configuration with n droplets will thus be smaller than the initial cylindrical configuration whenever

$$n < \frac{2}{9} \frac{L}{R}$$

with L/R large. We thus get a simple estimate of an upper bound on the number of droplets a jet can break into, however it is obvious that the configuration which minimises the surface energy is always obtained for $n = 1$, so that we have not explained why the jet breaks into more than one droplet.

If we assume that the slender jet equations of motion we have derived previously contain most of the physics necessary to explain the breakup phenomenon, a first step is to study the stability of some of the solutions of the system (9) and (10). The approach we will use is known generically as "linear stability analysis" and is applicable to many systems, but was pioneered by Rayleigh to study specifically what is now known as the "Rayleigh-Plateau" instability. The idea is to look for "wave-like" solutions of the form

$$
\begin{aligned}
h &= h_0 + \epsilon\,e^{ikz+\omega t} \\
u_0 &= \eta\,e^{ikz+\omega t}
\end{aligned}
\tag{11}
$$

where k is the wavenumber and ω is the "growth rate". The amplitude of the perturbations ϵ and η are also assumed to be small so that an asymptotic expansion in ϵ and η can be performed. These solutions can be injected into the momentum equation (9) which gives

$$
\begin{aligned}
\partial_t u_0 + u_0\,u_0' &= -\frac{\sigma}{\rho}\kappa' \\
\eta\,\omega\,e^{ikz+\omega t} + O(\eta^2) &= -\frac{\sigma}{\rho}\left(\frac{1}{h\,(1+h'^2)^{1/2}} - \frac{h''}{(1+h'^2)^{3/2}} \right)' \\
\eta\,\omega\,e^{ikz+\omega t} + O(\eta^2) &= -\frac{\sigma}{\rho}\left(-\frac{h'}{h^2} - h''' \right) + O(h'^2) \\
\eta\,\omega + O(\eta^2) &= \frac{\sigma}{\rho}\left(\frac{\epsilon\,i\,k}{h_0^2} - \epsilon\,i\,k^3 \right) + O(\epsilon^2)
\end{aligned}
\tag{12}
$$

where we have neglected both viscous effects and gravity. Doing the same with the kinematic boundary condition (10) gives

$$\partial_t h + \frac{1}{2}\,u_0'\,h + u_0\,h' + O(h^2) = 0$$

$$\epsilon\,\omega + \frac{1}{2}\,\eta\,i\,k\,h_0 + O(\epsilon^2) = 0$$

This can be used to eliminate ϵ in (12), which gives

$$\omega^2 = \frac{\sigma \, (k \, h_0)^2}{2 \, \rho \, h_0^3} \left(1 - k^2 \, h_0^2 \right) = \omega_0^2 \, x^2 \left(1 - x^2 \right) \tag{13}$$

with $x = k \, h_0$ the reduced wavenumber and $\omega_0^2 = \sigma/(2 \, \rho \, h_0^3)$. Thus we find that if $x = k \, h_0$ is larger than one, ω^2 is negative which corresponds to stable oscillatory solutions. On the other hand if x is smaller than one, ω is real and the perturbations grow exponentially with a growth rate given by (13). Figure 1 illustrates the dependence of the growth rate on the wave number. The most unstable wavenumber corresponds to $x = \sqrt{2}/2$.
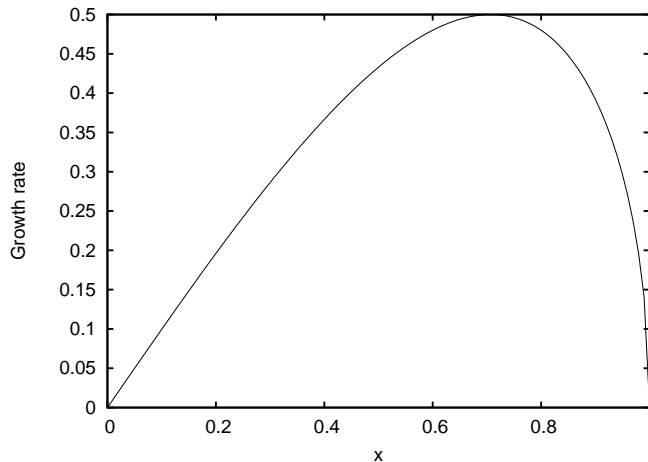
Figure 1. Growth rate ω/ω_0 as a function of the reduced wavenumber $x = k \, h_0$.

Note however that (13) is only an approximation of the full linear stability analysis. This is because the form of the perturbation we have taken in (11) is not volume-preserving in axisymmetric coordinates. A volume-preserving perturbation involves Bessel functions which complicates the analysis (see e.g. Eggers 1997 for the full analysis). The approximate solution in (13) is however quite good, with a maximum error on the growth rate of about 7% compared to the full solution. Using the full linear solution the most unstable wavenumber corresponds to $x \simeq 0.697$ which is indeed close to $\sqrt{2}/2$.

Is this result compatible with our earlier estimate on the maximum number of droplets n? If we assume that the number of droplets will be selected by the wavelength λ of the most unstable mode, we get

$$n = \frac{L}{\lambda}$$

with

$$\lambda = \frac{2 \, \pi}{k} = \frac{4 \, \pi \, R}{\sqrt{2}}$$

so that

$$n = \frac{\sqrt{2}}{4 \, \pi} \frac{L}{R} \simeq 0.113 \frac{L}{R}$$

which indeed verifies

$$n < \frac{2}{9} \frac{L}{R} \simeq 0.222 \frac{L}{R}$$

3 Singularities and self-similar solutions

We have identified the mechanism which causes a cylindrical column to break into droplets: the Rayleigh–Plateau instability. Our study was based, however, on linear stability analysis, which is only valid for small amplitudes of deformation. What happens closer to the point of breakup?

Figure 2 gives an example of the shape of the interface close to breakup in the case of a "dripping faucet" and a pulsating jet. This is clearly not well approximated by a (large amplitude) sine wave which suggests that non-linear effects are important. The asymmetry of the shape around the point of pinch-off is particularly striking. Note also that while one would be tempted to attribute the asymmetry to the influence of gravity, the same asymmetric shapes are also observed for the breakup of horizontal liquid jets. We will see later that gravity does not influence the breakup process.
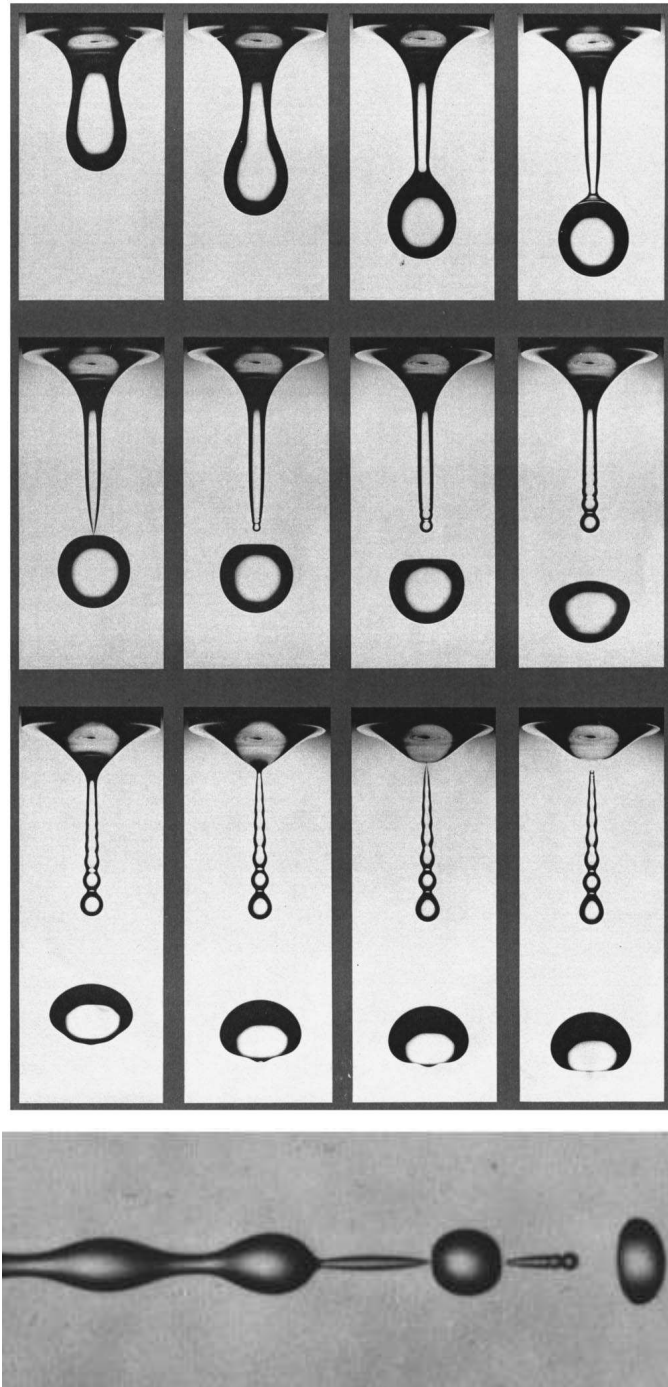
Figure 2. Top: Pinch-off of a droplet falling from a faucet. The asymmetry of the pinch-off shape is clearly visible on the 5th frame. Reproduced from Shi, Brenner and Nagel, 1994. Bottom: Breakup of a forced liquid jet. Reproduced from Rutland and Jameson, 1971. Note the similarity between the pinch-off in the 5th frame of the top figure and the first pinch-off in the bottom figure.

It is also clear from the experimental sequence (and from casual observation of droplets falling from faucets in e.g. kitchen sinks!) that the breakup process itself is much faster than the other processes involved (for example the overall shape of the droplet and liquid "column" barely changes between the 4th and 5th frames). This observation coupled to the apparent universality of the shape of the interface close to breakup (e.g. when comparing the faucet experiment with the breakup of forced liquid jets) leads to the intuition that the shape of the interface close to breakup must be independent of the initial conditions. If this is the case, the solution for the shape of the interface cannot depend on length scales characteristic of the initial conditions (for example the initial diameter for jet breakup, or the diameter of the tap for the faucet experiment). In addition, since by definition the jet radius tends toward zero close to breakup, the solution does not admit any obvious dimensioning length scale and it becomes natural to look for universal solutions characterised by *scale invariance* i.e. self-similar solutions which are invariant when rescaling the spatial coordinates appropriately.

To look for these solutions, we will start from the simplified system of one-dimensional equations derived previously (equations (9), (10) and (7))

$$\partial_t u + u\,u' \;=\; -\frac{\sigma}{\rho}\,k' + 3\,\frac{\mu}{\rho}\,\frac{(u'\,h^2)'}{h^2} - g$$
$$\partial_t h + u\,h' \;=\; -\frac{1}{2}\,u'\,h$$

These equations are written in dimensional form and as such depend implicitly on length scales characteristic of the initial conditions. A first step is to rescale them using length and timescales relevant close to breakup. When we exclude the length and timescales associated with the initial conditions, the only remaining dimensional quantities are the material parameters:

- viscosity μ, dimension of mass $\times$ length^{-1} $\times$ time^{-1}
- density ρ, dimension of mass $\times$ length^{-3}
- surface tension coefficient σ, dimension of mass $\times$ time^{-2}

It is simple to show that the only timescale which can be constructed using a combination of these parameters is the viscous–capillary timescale

$$t_\nu = \frac{\mu^3}{\sigma^2\,\rho}$$

Similarly the only possible length scale is

$$l_\nu = \frac{\mu^2}{\sigma\,\rho}$$

These time and length scales can be interpreted physically as the characteristic time (resp. length) over which capillary forces are balanced by viscous forces. For example, for water $l_\nu \simeq$ 13.9 nanometers and $t_\nu \simeq 1.91 \times 10^{-10}$ seconds while for glycerin, $l_\nu \simeq 2.79$ centimeters and $t_\nu \simeq$ 0.652 seconds.

Using these length and timescale, we can introduce the rescaled space and time coordinates

$$\bar{z} = \frac{z - z_0}{l_\nu} \qquad \text{and} \quad \bar{t} = \frac{t - t_0}{t_\nu}$$

where t_0 and z_0 are the time and location of the pinch-off respectively. If we also introduce the rescaled velocity and radius $\bar{u}$ and $\bar{h}$ such that

$$u(z,t) = \frac{l_\nu}{t_\nu}\,\bar{u}\,(\bar{z},\bar{t}\,) \quad \text{and} \quad h(z,t) = l_\nu\bar{h}\,(\bar{z},\bar{t}\,)$$

the simplified equations of motion can then be rewritten

$$-\partial_{\bar{t}}\bar{u} + \bar{u}\,\bar{u}\,' \;=\; -\bar{\kappa}' + 3\,\frac{(\bar{u}\,'\bar{h}\,^2)'}{\bar{h}\,^2} - \bar{g}$$
$$-\partial_{\bar{t}}\bar{h} + \bar{u}\,\bar{h}\,' \;=\; -\frac{1}{2}\,\bar{u}\,'\bar{h}$$

with

$$\bar{g} = g\,\frac{t_\nu^2}{l_\nu}$$

Note that as expected the rescaled set of equations is free of any independent parameter.

As mentioned previously, we now look for solutions of these equations which are scale-invariant i.e. which take the general form

$$\bar{h}(\bar{z},\bar{t}) = \bar{t}^{\,\alpha_1}\phi(\xi)$$
$$\bar{u}(\bar{z},\bar{t}) = \bar{t}^{\,\alpha_2}\psi(\xi)$$

with α_1 and α_2 scaling exponents to be found, ϕ and ψ the generic "shape functions" also to be found and

$$\xi = \frac{\bar{z}}{\bar{t}^{\,\beta}}$$

the "similarity variable" with β another scaling exponent also to be found. The exponents α_1, α_2 and β describe how the radial dimension, axial velocity and longitudinal dimension respectively need to be rescaled in time to obtain the invariant solutions described by functions ϕ and ψ.

As in the previous section the derivative of the curvature in axisymmetric coordinates can be approximated by

$$\bar{\kappa}' = -\frac{\bar{h}'}{\bar{h}^2} - \bar{h}''' + O(\bar{h}'^2)$$

in the case of slender jets. Close to breakup this can be further simplified by noting that the mean curvature will be dominated by the curvature component normal to the (r, z) plane so that the third derivative $\bar{h}'''$ becomes negligible in the expression above. Using this approximation and injecting the scale-invariant forms into the equations of motion, we have

$$\bar{h}'(\bar{z},\bar{t}) = \bar{t}^{\,\alpha_1-\beta}\phi'(\xi)$$
$$\bar{u}'(\bar{z},\bar{t}) = \bar{t}^{\,\alpha_2-\beta}\psi'(\xi)$$

and thus

$$-(\alpha_2\,\bar{t}^{\,\alpha_2-1}\psi - \bar{t}^{\,\alpha_2}\beta\xi\,\bar{t}^{\,-1}\psi') + \bar{t}^{\,\alpha_2}\psi\,\bar{t}^{\,\alpha_2-\beta}\psi' = \frac{\bar{t}^{\,\alpha_1-\beta}\phi'}{\bar{t}^{\,2\alpha_1}\phi^2} + 3\frac{\bar{t}^{\,2\alpha_1+\alpha_2-2\beta}(\psi'\phi^2)'}{\bar{t}^{\,2\alpha_1}\phi^2} - \bar{g}$$

$$-(\alpha_1\,\bar{t}^{\,\alpha_1-1}\phi - \bar{t}^{\,\alpha_1}\beta\xi\,\bar{t}^{\,-1}\phi') + \bar{t}^{\,\alpha_2}\psi\,\bar{t}^{\,\alpha_1-\beta}\phi' = -\frac{1}{2}\bar{t}^{\,\alpha_2-\beta}\psi'\,\bar{t}^{\,\alpha_1}\phi \qquad (14)$$

To find the exponents α_1, α_2 and β we will assume that all terms in the momentum equation (the first equation above) play a role arbitrarily close to breakup (i.e. when $\bar{t} \to 0$). These terms correspond to: on the left-hand-side, inertia and on the right-hand-side: surface tension and viscosity (we will talk later about gravity). This means that the exponents of $\bar{t}$ appearing in front of these terms must be identical, which gives the relations

$$\alpha_2 - 1 = \alpha_2 - 1 = 2\alpha_2 - \beta = -\alpha_1 - \beta = \alpha_2 - 2\beta$$

This system has for solution

$$\beta = \frac{1}{2} \quad \alpha_1 = 1 \quad \alpha_2 = -\frac{1}{2}$$

We need to check that this solution is also consistent with the continuity equation (14) i.e. the different terms in this equation must also be of the same order when $\bar{t} \to 0$ which gives

$$\alpha_1 - 1 = \alpha_1 - 1 = \alpha_2 + \alpha_1 - \beta = \alpha_2 + \alpha_1 - \beta$$

which is also verified.

The self-similar solution thus verifies the following scalings

$$\bar{h}(\bar{z},\bar{t}) = \bar{t}\,\phi\!\left(\frac{\bar{z}}{\bar{t}^{\frac{1}{2}}}\right)$$

$$\bar{u}(\bar{z},\bar{t}) = \bar{t}^{-\frac{1}{2}}\psi\!\left(\frac{\bar{z}}{\bar{t}^{\frac{1}{2}}}\right)$$

The radius decreases linearly with time and the velocity diverges as the inverse of the square root of time. Similarly all the terms in the momentum equation diverge as $\bar{t}^{-3/2}$ and dominate the (constant) gravity close to the singularity. Note also that this solution is a true singularity of the Navier–Stokes equations since all the terms where retained. In particular, one could expect viscosity to "regularise" the singularity, however this is clearly not the case here.

Can we say more about the shape of the solution close to the singularity? With this choice of exponents, the powers of time drop out of equations (14) and the shape functions ϕ and ψ must verify

$$\frac{1}{2}\psi + \frac{1}{2}\xi\psi' + \psi\psi' = \frac{\phi'}{\phi^2} + 3\frac{(\psi'\phi^2)'}{\phi^2} \tag{15}$$

$$-\phi + \frac{1}{2}\xi\phi' + \psi\phi' = -\frac{1}{2}\psi'\phi \tag{16}$$

To be able to solve for ϕ and ψ in this system of coupled ordinary differential equations, we also need enough boundary conditions. The system involves the first derivatives of ϕ and ψ and the second derivative of ψ so that we need three boundary conditions. We can find these conditions by "matching" the solution close to pinch-off with the solution far from the singularity (i.e. for $\bar{z} \to \pm\infty$). In particular, far enough from the singularity the velocity and radius must become independent from time which implies

$$\phi(\xi) \to \bar{t}^{-1} \quad \text{for} \quad \xi \to \pm\infty$$
$$\psi(\xi) \to \bar{t}^{\frac{1}{2}} \quad \text{for} \quad \xi \to \pm\infty$$

or equivalently, using the definition of ξ

$$\phi(\xi) \to \xi^2 \quad \text{for} \quad \xi \to \pm\infty$$
$$\psi(\xi) \to \xi^{-1} \quad \text{for} \quad \xi \to \pm\infty$$

The third boundary condition is much more difficult to obtain and we refer the reader to Eggers and Dupont, 1994 and Brenner, Lister and Stone, 1996 for a detailed discussion. With these boundary conditions, the system of ODEs (15) and (16) can be solved numerically. This gives the universal solutions depicted on Figure 3. As observed in experiments, the solutions are very asymmetric.
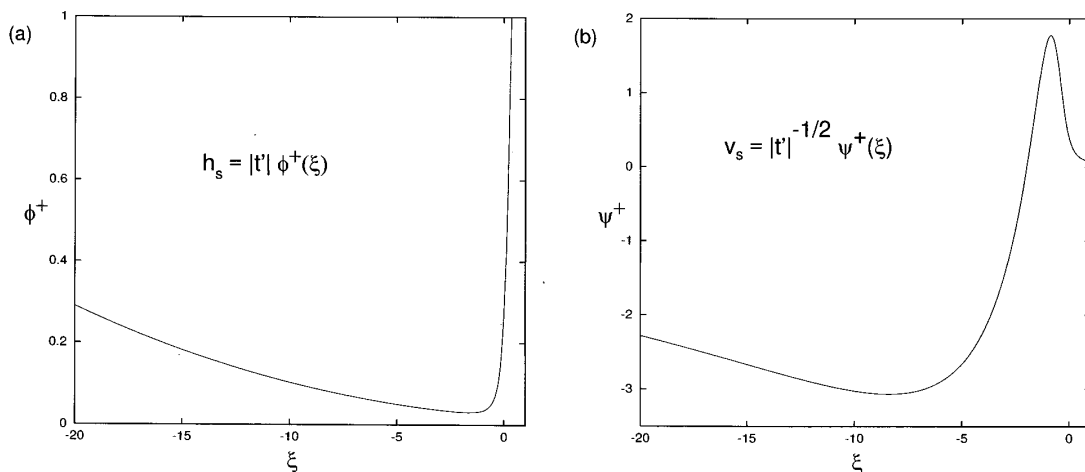
Figure 3. Similarity functions ϕ and ψ. Reproduced from Eggers, 1997.

3.1   Scalings far from the singularity

The solutions derived previously are only valid close enough to the singularity (and far enough from the initial conditions). In particular, by construction, they are only valid when surface tension forces are comparable to viscous forces i.e. when the relevant spatial scales (e.g. the radius of the jet) are comparable to the viscous–capillary length scale l_ν. As we have seen before, for some usual liquids (such as water), l_ν is extremely small so that most of the observable breakup process will not be described by the viscous self-similar solutions. In this regime, the dynamics are dominated by surface tension and inertia and viscosity is negligible.

If viscosity is neglected, we cannot use the characteristic time and length scales l_ν and t_ν to measure the distance to the singularity. The natural units are then the outer length scale L_0 (the initial radius of the jet) and the corresponding timescale

$$T_0 = \sqrt{\frac{\rho L_0^3}{\sigma}}$$

The rescaled space and time coordinates thus become

$$\bar{z} = \frac{z - z_0}{L_0} \quad \text{and} \quad \bar{t} = \frac{t - t_0}{T_0}$$

with the rescaled velocity and radius

$$u(z,t) = \frac{L_0}{T_0}\,\bar{u}\,(\bar{z},\bar{t}\,) \quad \text{and} \quad h(z,t) = L_0\,\bar{h}\,(\bar{z},\bar{t}\,)$$

The inviscid simplified equations of motion are then rescaled as

$$
\begin{aligned}
-\partial_{\bar{t}}\bar{u} + \bar{u}\bar{u}\,' &= -\bar{k}\,' - \bar{g} \\
-\partial_{\bar{t}}\bar{h} + \bar{u}\,\bar{h}\,' &= -\frac{1}{2}\,\bar{u}\,'\bar{h}
\end{aligned}
$$

with

$$\bar{g} = g\,\frac{T_0^2}{L_0}$$

Looking for self-similar solutions as in the previous section i.e.

$$
\begin{aligned}
\bar{h}\,(\bar{z},\bar{t}\,) &= \bar{t}^{\,\alpha_1}\,\phi_i(\xi) \\
\bar{u}\,(\bar{z},\bar{t}\,) &= \bar{t}^{\,\alpha_2}\,\psi_i(\xi) \\
\xi &= \frac{\bar{z}}{\bar{t}^{\,\beta}}
\end{aligned}
$$

we now get the under-determined system of equations

$$\alpha_2 - 1 = 2\,\alpha_2 - \beta = -\alpha_1 - \beta$$

$$\alpha_1 - 1 = \alpha_2 + \alpha_1 - \beta = \alpha_2 + \alpha_1 - \beta$$

which admits the family of solutions

$$\alpha_1 = 2 - 2\,\beta \qquad \alpha_2 = \beta - 1$$

An interesting particular case is $\beta = 2/3$ for which the similarity variable ξ becomes

$$\xi = \frac{\bar{z}}{\bar{t}^{\,\beta}} = \frac{z - z_0}{(t - t_0)^{2/3}}\,\frac{T_0^{2/3}}{L_0} = \frac{z - z_0}{(t - t_0)^{2/3}}\left(\frac{\rho}{\sigma}\right)^{1/3}$$

In the same manner the solution for the radius and velocity become

$$h(z,t) = L_0\,\bar{h}\,(\bar{z},\bar{t}\,) = L_0\,\bar{t}^{\,2/3}\,\phi_i(\xi) = L_0\,\frac{(t-t_0)^{2/3}}{T_0^{2/3}}\,\phi_i(\xi) = \left(\frac{\sigma}{\rho}\right)^{1/3}(t - t_0)^{2/3}\,\phi_i(\xi)$$

$$u(z,t) = \frac{L_0}{T_0}\,\bar{u}\,(\bar{z},\bar{t}\,) = \frac{L_0}{T_0}\,\bar{t}^{\,-1/3}\,\psi_i(\xi) = \frac{L_0}{T_0}\,\frac{(t-t_0)^{-1/3}}{T_0^{-1/3}}\,\psi_i(\xi) = \left(\frac{\sigma}{\rho}\right)^{1/3}(t - t_0)^{-1/3}\,\psi_i(\xi)$$

so that the solution becomes entirely independent from the outer length scale L_0. Note however that a fundamental difference between this solution and the solution obtained in the viscous limit is that we do not have an explanation of why this particular (convenient) exponent should be selected in practice. We can only wave our hands and say that we expect a valid inviscid solution to "forget" the initial conditions (and thus L_0) when getting closer to breakup.

Finally the table below summarises the results we have obtained for the viscous and inviscid breakup solutions.

	viscous	inviscid
ξ	$l_\nu^{-1} t_\nu^{1/2} (t-t_0)^{-1/2} (z-z_0)$	$\left(\frac{\sigma}{\rho}\right)^{-1/3} (t-t_0)^{-2/3} (z-z_0)$
$h(z,t)$	$l_\nu t_\nu^{-1} (t-t_0)\, \phi(\xi)$	$\left(\frac{\sigma}{\rho}\right)^{1/3} (t-t_0)^{2/3}\, \phi_i(\xi)$
$u(z,t)$	$l_\nu t_\nu^{-1/2} (t-t_0)^{-1/2}\, \psi(\xi)$	$\left(\frac{\sigma}{\rho}\right)^{1/3} (t-t_0)^{-1/3}\, \psi_i(\xi)$

Table 1. Viscous and inviscid similarity solutions.

Bibliography

[1] M.P. Brenner, J.R. Lister, and H.A. Stone. Pinching threads, singularities and the number 0.0304... *Physics of Fluids*, 8(11):2827–2836, 1996.

[2] J. Eggers. Nonlinear dynamics and breakup of free-surface flows. *Reviews of Modern Physics*, 69(3):865, 1997.

[3] J. Eggers and T.F. Dupont. Drop formation in a one-dimensional approximation of the Navier–Stokes equation. *Journal of fluid mechanics*, 262(-1):205–221, 1994.

[4] J.B. Keller and M.J. Miksis. Surface tension driven flows. *SIAM Journal on Applied Mathematics*, 43(2):268–277, 1983.